

**IMPROVED β - γ COINCIDENCE DETECTOR
FOR RADIOXENON DETECTION**

Matthew W. Cooper, April J. Carman, James C. Hayes, Tom R. Heimbigner, Charles W. Hubbard, Kevin E. Litke, Justin I. McIntyre, Scott J. Morris, Michael D. Ripplinger, and Reynold Suarez

Pacific Northwest National Laboratory

Sponsored by National Nuclear Security Administration
Office of Nonproliferation Research and Engineering
Office of Defense Nuclear Nonproliferation

Contract No. DE-AC06-76RL01830

ABSTRACT

The Automated Radioxenon Analyzer/Sampler (ARSA), built by Pacific Northwest National Laboratory (PNNL), can collect and detect several radioxenon isotopes. ARSA is very sensitive to ^{133}Xe , $^{131\text{m}}\text{Xe}$, $^{133\text{m}}\text{Xe}$ and ^{135}Xe due to the compact high efficiency β - γ coincidence detector it uses. For this reason it is an excellent treaty monitoring and environmental sampling device. Although the system is shown to be both robust and reliable, based on several field tests, it is also complex due to a detailed photomultiplier tube gain matching regime. This complexity is a problem from a maintenance and quality assurance/quality control (QA/QC) standpoint. To reduce these issues a simplified β - γ coincident detector has been developed. A comparison of three different well detectors has been completed. In addition, a new plastic scintillator gas cell was constructed. The new simplified detector system has compared favorably with the original ARSA design in spectral resolution and efficiency and is significantly easier to setup and calibrate.

OBJECTIVES

Monitoring radioactive releases from nuclear explosions is a major component of the International Monitoring System [1]. As part of the international effort to develop monitoring equipment PNNL developed and deployed two automated units. The first system developed was the Radionuclide Aerosol Sampler/Analyzer (RASA), which has been deployed at over 30 locations. The RASA collects airborne radioactive particulate debris on filters, which are then counted with a high purity germanium (HPGe) detector [2]. The second system, the Automated Radioxenon Analyzer/Sampler (ARSA)[3], measures radioxenon isotopes by directly collecting and processing air samples. The radioxenon isotopes are generated in nuclear fission, and the isotopic ratios can be used to distinguish the xenon generated in power reactors from that generated in nuclear explosions. The specific isotopes are identified and measured using either the β - γ coincidences or the conversion electron (CE) and x-ray coincidences [4].

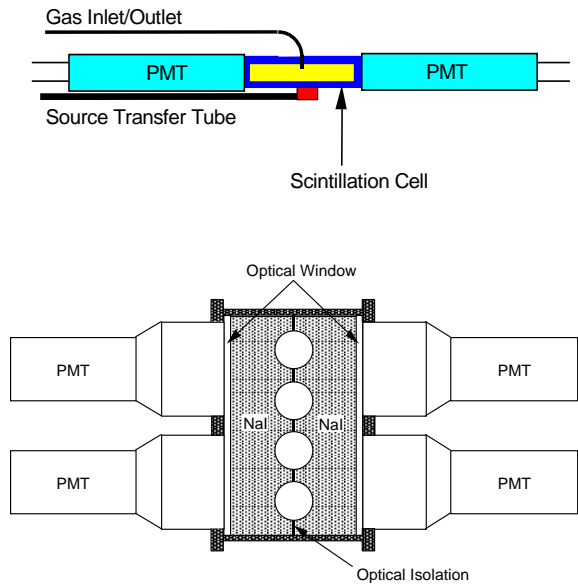


Figure 1. Upper schematic is a representation of the plastic scintillation gas cell with photo-multiplier tubes (PMT), gas transfer line and calibration source transfer tube. The lower schematic is a diagram of the NaI(Tl) γ detector. Plastic scintillator β cells occupy the four holes in the NaI(Tl) detectors. These holes extend all the way through the detector.

In the ARSA, a low background NaI(Tl) detector measures the photon energy and a plastic scintillation gas cell (Figure 1) detects the charged particles. The optimum CE and β energy resolution is achieved by viewing the 5 cm long gas cell on either end by gain matched 15-mm photo-multiplier tubes (PMT). The gas cell has a nearly 100% efficiency due to 4π coverage, although there is a small loss due to the low energy of the β coming from ^{133}Xe and ^{135}Xe as well as the standard losses associated with light transmission in a scintillator. The gas cells are enclosed in four transverse NaI(Tl) wells, which provide very good solid angle coverage for emitted γ - and x-rays while still maintaining a compact unit. The two independent NaI(Tl) crystals allow rejection of multiple scatter and background events; however gain matching the PMTs is also difficult and time consuming. To eliminate gain matching, the number of PMTs can be reduced. However, given a reduction in the PMT number, it is still necessary to maintain a large solid angle ($>3.5\pi$ coverage) for β - γ nuclear emissions, an adequate energy resolution, a robust scintillation material for field use, and minimal attenuation of x-rays and low energy γ -rays.

Experimental Apparatus

The new design uses a single well detector to detect the x-rays and γ -rays, along with a single PMT gas cell to detect the β and CE emissions. The first diagram in Figure 2 is a rendering of the complete 4 gas cell detector assembly, which includes individual CsI(Na) wells, gas cells, surrounding copper, and 2.5 cm thick lead cave. The well detectors are tightly packed to help reject both cosmic-rays and ambient γ -rays in the same fashion as the original ARSA detector. The second diagram shows the internal layout of the gas cell and PMT with a high-voltage tube base. The gas cell is 28 mm long by 18 mm in diameter with 2 mm thick plastic scintillation walls and a rounded end. A stepped plastic end-cap closes the gas cell and a small hole provides for a thin gas transfer tube. This redesign accomplished several critical goals, which include: simplified calibration, increased robustness, and increased efficiency. The reduction in the initial setup calibration efforts is directly attributed to each of the four γ -ray detectors being able to be calibrated independently. The new detector is more robust since each cell is separate from the others, which in effect eliminates the effect a poor energy or resolution response from a defective PMT has on the other detectors. Finally, the overall detection efficiency has improved with the increase of the solid angle of detection. The gas cell energy resolution was maintained, despite the reduction to one PMT, by using a larger PMT and by rounding the ends of the gas cells.

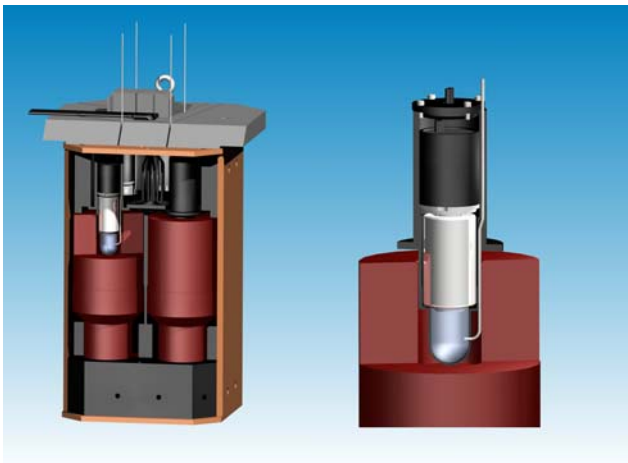


Figure 2. Schematic of four well detectors with gas cells, inside of 1" lead cave. The second schematic is the redesigned gas cell with PMT and tube base. The cell extends 5.5 cm into the CsI(Na) wells to provide the same solid angle coverage as the ARSA gas cells.

RESEARCH ACCOMPLISHED

γ -ray Detectors

Using the new design, studies were performed to replicate and possibly enhance the performance of the γ -ray and gas cell β detectors. Furthermore, a new more robust scintillation material was sought to replace the NaI(Tl). Cesium Iodide doped with Na or Tl were two obvious choices. Cesium Iodide has comparable density, detection efficiency, energy resolution, light output, and timing characteristics with NaI(Tl) but is much more robust. Three well detectors, a NaI(Tl), a CsI(Tl) and a CsI(Na), were procured differing only in the material [5]. The crystal sizes were a right cylinder 7.6 cm long by 8.13 cm in diameter, with a 3.1 cm wide by 5.1 cm deep well. The three well detectors were initially compared for resolution and relative efficiency. The 7.5 cm diameter PMTs were optically matched to maximize the total response for the characteristic wavelength emission of each type of crystal. Initial studies included energy response linearity, energy resolution, and efficiency across a wide range of x-ray and γ energies. Figure 3 shows the spectrum obtained with the CsI(Tl) using a multi-line γ -ray standard from Amersham[®]. The linearity of the energy calibration was excellent for the three detectors, however the CsI detectors were markedly better

across the entire range, see Table 1. The ^{137}Cs γ line at 661.7 keV was used to compare the resolution and efficiency for the three detectors.

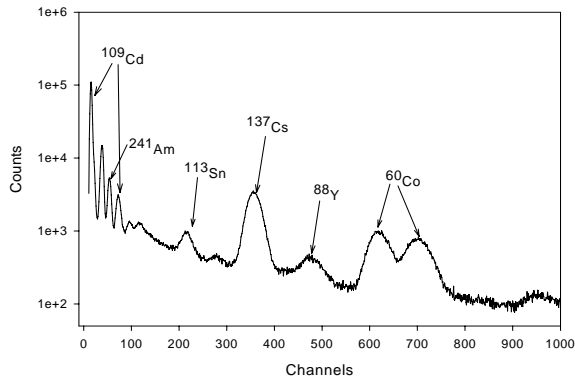


Figure 3. Histogram of the CsI(Tl) response using an Amersham[®] radiological standard. The energy range covers the 22 keV x-ray from ^{109}Cd to the double peaks at 1179 keV and 1332 keV of ^{60}Co . Each peak was fit with a Gaussian using SigmaPlot[®] to determine the peak centroid and the peak width.

Table 1. γ Detector Comparison

Parameters	γ Detector Material		
	NaI(Tl)	CsI(Na)	CsI(Tl)
Quadratic term / linear term	7.4×10^{-4}	5.8×10^{-5}	1.7×10^{-4}
Resolution @ 661.7 keV (%)	6.7 ± 0.1	8.7 ± 0.1	9.5 ± 0.1
Relative efficiency @ 661.7 keV (%)	24.2 ± 1.0	28.3 ± 1.2	28.1 ± 1.4
Density (g/cm^3) [5]	3.67	4.51	4.51
Primary decay time (ns) [5]	230	630	1000

As expected, the NaI(Tl) had the best resolution of the three detectors due to the better optical matching of the PMT to the NaI(Tl) scintillation light emissions. The primary x-rays and γ -rays of interest are at 30 keV, 80 keV and 250 keV, which have large enough energy separations that the CsI crystals were more than adequate for good resolving power between the peaks. Also expected is the increase in efficiency seen by the two CsI crystals. They have densities that are $\sim 23\%$ greater than NaI and the average electron density is $\sim 20\%$ greater.

Gas Cell Detectors

The ARSA gas cells need to discriminate between the two conversion electrons of $^{133\text{m}}\text{Xe}$ and $^{131\text{m}}\text{Xe}$ and the β distributions from ^{133}Xe (see Table 2 for the primary decay paths for each of the radioxenons). The original ARSA gas cells had two PMTs looking at either end of the 1.5 cm x 5 cm right cylinder cell with 1.2 mm thick walls. By gain matching photo-tubes, a 25-30% resolution for the 129 keV CE can be achieved. A major requirement for the new simplified scintillator gas cell was that it needs to attain a similar resolution to the ARSA beta cells. The material choices for the gas cells were limited to materials that were non-hygroscopic, had good charged particle energy resolution, were robust, and were sufficiently thin such that the walls did not attenuate the 30 keV x-rays from ^{133}Xe , $^{131\text{m}}\text{Xe}$ and $^{133\text{m}}\text{Xe}$. The ARSA detector employed BC-404 scintillating plastic shaped into hollow tubes with stepped end caps to complete a gas tight cell [5]. The new gas cell has slightly thicker walls and end cap and were molded into a concave shape. This design allows for only one PMT to be used on the plastic scintillator. Light is refocused from the rounded end back towards the single PMT. The overall dimensions were 2 mm thick and 28 mm long. A larger PMT was used to maximize the use of the sensitive central portion of the PMT where the conversion efficiency is highest. To enhance the internal reflection of light back towards the PMT the gas cell was wrapped in two layers of Teflon tape. The effect of the Teflon tape can clearly be seen in Figure 4

which shows the response of the plastic gas cell to a ^{36}Cl β source. Several β sources were used for this study and only the ^{36}Cl is shown to illustrate the additional light collection that the Teflon provides.

Table 2. Dominant Decay Modes of the Radioxenon Isotopes ^a.

Isotope	$^{131\text{m}}\text{Xe}$	^{133}Xe	$^{133\text{m}}\text{Xe}$	^{135}Xe
Half-life (days)	11.84	5.24	2.19	0.38
Primary γ -ray energy (keV)	163.9	81.0	233.2	249.8
γ -ray abundance (%)	1.96	37	10.3	90
X-ray energy (keV)	30	31	30	31
X-ray abundance (%)	54	48.9	56.3	5.2
β -particle endpoint energy (keV)	346	905		
β -particle abundance (%)	99	96		
Conversion electron energy (keV)	129	45	199	214
Conversion electron abundance (%)	60.7	54	63.1	5.7

^a From Ref. [6].

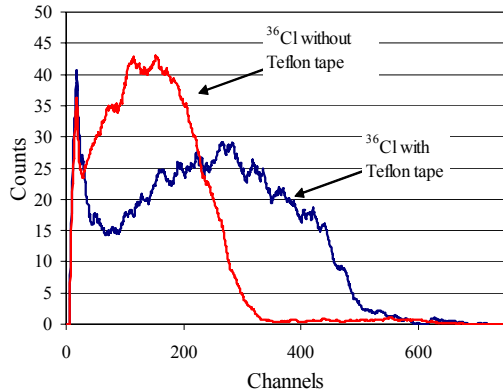


Figure 4. Response of the new gas cell with and without the Teflon tape wrapping. It is clear that the addition of the Teflon reflector provides a significant increase in the total light collected by the PMT. The source used is ^{36}Cl with a β end point energy of 1142 keV. The full energy is unlikely to be deposited because the 2 mm thick plastic has a stopping power of ~ 450 keV.

β - γ Coincidence Measurements

Two tests were performed using the new gas cell and three well detectors to compare performance characteristics between the different detector types. The first test uses Compton scattering of the 662 keV peak from ^{137}Cs to generate β - γ coincidences in the detector, see reference 8 for an in-depth description of the technique. The second technique uses well-aged radioxenon from a commercial medical isotope supplier. This source has both ^{133}Xe and $^{131\text{m}}\text{Xe}$, the metastable is a contaminant at very low relative levels compared to the ^{133}Xe after several months the metastable has decayed much less and is therefore more abundant and easily discernable in the mixed source. The initial source strength (174 MBq) is far too high to use and aging has the effect of decreasing the ^{133}Xe activity down to useable levels.

Compton Scattering Technique Using ^{137}Cs

The use of Compton scattering of γ -rays is a very successfully technique and provides a method of β -energy and energy resolution calibration that can be done quickly and in the case of the ARSA system automatically and remotely. It provides a reliable method to compare detector response over an extended period. It also allows gain shifts in PMT and relative efficiency declines to be measured and tracked. The technique allows a more direct measurement than using β sources because the γ -rays illuminate the entire

gas cell, therefore eliminating much of the position dependence of the source. The typical β sources illuminate only the material directly in front of the source. Assuming only Compton scatter occurs (low atomic numbers in the plastic prevent gamma-ray absorption from occurring with any measurable frequency), the maximum energy transfer to an electron is 477 keV. Within the β - γ coincidence plane all electron energies from 0 to 477 keV would be populated. Figure 5 is a 2-dimensional β - γ histogram that clearly shows the Compton electrons that are scattered in the plastic of the gas cell and scattered γ -ray. The diagonal line is along constant energy when the γ energy is added to the β energy: $E_{\beta} + E_{\gamma} = 662$ keV.

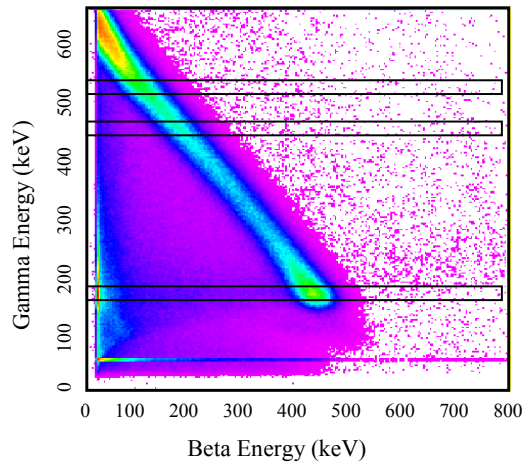


Figure 5. This plot shows the 2-dimensional β - γ coincidence histogram using a ^{137}Cs source. The diagonal feature is a constant energy line from the 662 keV γ -ray from ^{137}Cs and indicates Compton scattering. The γ endpoint is at 662 keV and the β endpoint is at 477 keV. Intermediate values can be used to define the β energy scale and the resolution of the gas cell.

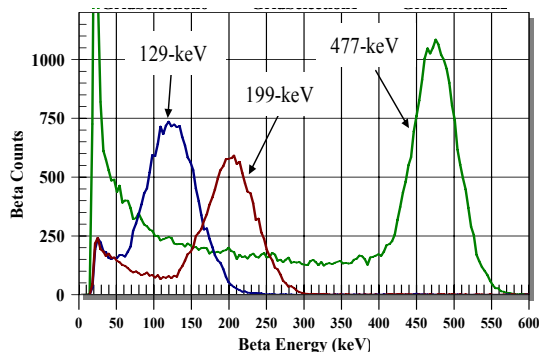


Figure 6. Highlighting narrow regions in the β - γ histogram (Figure 5) at the appropriate γ energies gives a projection along the β axis that is centered at the CE energies of $^{131\text{m}}\text{Xe}$, $^{133\text{m}}\text{Xe}$ and the Compton scatter endpoint energy of 477 keV for the 662 keV γ from ^{137}Cs .

This correlation gives the β energy scale when the γ energy scale is calculated using the Amersham[®] source. It also allows the determination of the β energy resolution from ~ 15 keV all the way up to 477 keV. Figure 6 shows the results of this analysis for the Compton scattered equivalent CE energies of $^{131\text{m}}\text{Xe}$ and $^{133\text{m}}\text{Xe}$ as well as the Compton scattering endpoint. The fit of the Gaussian peaks along the constant energy line is an indication of how linear the detector response is. In the ARSA gas cell,

comparable linearity was achieved only by tedious and time consuming PMT matching and taking the geometric sum of the response of the two PMTs. The overlap between the 129 keV and 199 keV peaks is $\sim 10\%$. While it is possible to determine through peak fitting routines the counts in each of these peaks, it would be beneficial if this overlap were reduced further. The β energy resolution for the new detector using one PMT is equivalent to the ARSA detector using two. Thus there is no loss of detector performance.

Radioxenon Response

The use of aged medical ^{133}Xe gives a direct measure of the β energy and resolution as well as providing the complete response of the β - γ coincidence detector. Figure 7 shows the 2-dimensional β - γ coincidence spectrum that was obtained after injecting a well aged ^{133}Xe sample with $^{131\text{m}}\text{Xe}$ as a contaminate. The plot shows the two regions for ^{133}Xe highlighted. The $^{131\text{m}}\text{Xe}$ shows up as a dark spot in the 30 keV x-ray region. The inset shows the projection of the data to the γ -axis and indicates the excellent separation between the x-ray and γ -ray response. The 30 keV x-rays of the ^{133}Xe and the $^{131\text{m}}\text{Xe}$ are indistinguishable along this axis and show the power of using the β energy and CE energy in coincidence. Figure 8 shows the projection of the two regions on the β axis. The 80 keV region is a pure ^{133}Xe β distribution with no CE interferences. The x-ray region has two CE, one at 45 keV for the ^{133}Xe (small peak) and the more prominent CE is centered at 129 keV and is from the decay of $^{131\text{m}}\text{Xe}$. The resolution of this peak is 0.248 ± 0.031 , which is in very good agreement with the ARSA detector.

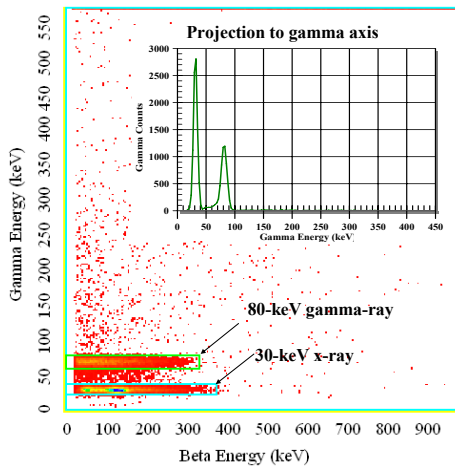


Figure 7. This plot shows the 2-dimensional beta-gamma coincidence histogram of a ^{133}Xe plus $^{131\text{m}}\text{Xe}$ gas. The two regions for ^{133}Xe are highlighted and the $^{131\text{m}}\text{Xe}$ shows up as a dark spot in the x-ray region. The inset shows the projection of the data to the γ -axis and indicates the excellent separation between the x-ray and γ -ray response.

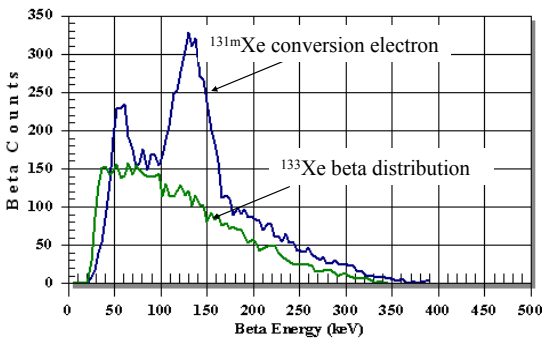


Figure 8. The projection of the two regions marked in Figure 7 are indicated above. The γ -ray region is a pure ^{133}Xe β distribution with no CE interferences. The x-ray region has two CE, one at 45 keV for the ^{133}Xe (small peak) and the more prominent CE is centered at 129 keV and is from the decay $^{131\text{m}}\text{Xe}$. The resolution of this peak is 0.248 ± 0.031 , which is in good agreement with the ARSA detector.

CONCLUSIONS AND RECOMMENDATIONS

The optimal replacement well detector was determined to be CsI(Na), because it has good mechanical properties and better efficiency than the NaI(Tl). It also has a time decay constant that is closer to that of NaI(Tl) than the longer CsI(Tl), so it has less impact on the readout electronics. Likewise, the gas cell redesign gives comparable results in linear energy response and resolution to the multi-PMT configuration. The new geometry also has helped to reduce the energy calibration time and complexity and now can be done using automated operation and analysis routines. The failure of one detector has a much lower impact on the other detectors due to the new design.

Two future studies that are needed before a true replacement detector can be fielded in the ARSA units are the effect the close pack detector design has on vetoing cosmic-rays and an extended period of testing under field conditions.

The new detector design is much easier to calibrate and allows in-field replacement of a single unit. Initial studies indicated that the well design maintains both radioxenon detection efficiency and γ -ray energy resolution. Furthermore, the design has the potential to be an excellent replacement β - γ coincidence detector system for the fielded ARSA system.

REFERENCES

- [1] Operational manual for radionuclide and the international exchange of radionuclide data, preparatory commission for the Comprehensive Nuclear-Test-Ban-Treaty Organization, CTBT/WGB/TL-11/5/Rev. 4, (1999).
- [2] Miley, H. S, R. J. Arthur., E. A. Lepel, S. L. Pratt, and C. W. Thomas (2001). "Evaluation of fission product isotopes for field or laboratory detection", *Jour. Radioanalytical Chemistry*, Vol. 248-3, pp. 651-656, June.
- [3] Hayes, James C., Keith H. Abel, Theodore W. Bowyer, Tom R. Heimbigner, Mark E. Panisko, Paul L. Reeder, Justin I. McIntyre, Robert C. Thompson, Lindsay C. Todd, Ray A. Warner (1999). Operations of the automated Radioxenon sampler/analyzer - ARSA, in the *Proceedings of the 21st Seismic Research Symposium: Technologies for Monitoring the Comprehensive Nuclear-Test-Ban Treaty*, LA-UR-99-4700, Vol. 2, pp. 249-260.
- [4] Bowyer, T. W., J.I. McIntyre, and P. Reeder (1999). High sensitivity detection of Xe isotopes via β - γ coincidence counting, in the *Proceedings of the 21st Seismic Research Symposium: Technologies for Monitoring the Comprehensive Nuclear-Test-Ban Treaty*, LA-UR-99-4700, Vol. 2, pp. 231-241.
- [5] Saint Gobain© website, <http://www.bicron.com/>
- [6] Browne, E., and R.B. Firestone (1986). *Table of Radioactive Isotopes*, Wiley, New York.